Combination of statistical and physically-based methods to assess shallow slides susceptibility at the basin scale

Sérgio C. Oliveira[1], José L. Zêzere[1], Sara Lajas[1],Raquel Melo[1]

[1]Centre for Geographical Studies, IGOT (Institute of Geography and Spatial Planning), Universidade de Lisboa, Edifício IGOT, Rua Branca Edmée Marques, 1600-276 Lisboa, Portugal

Correspondence to: Sérgio C. Oliveira (cruzdeoliveira@campus.ul.pt)

Abstract. Approaches used to assess shallow slides susceptibility at the basin scale are conceptually different depending on the use of statistical or physically-based methods. The former are based on the assumption that the same causes are more likely to produce the same effects, whereas the latter are based on the comparison between forces which tend to promote movement along the slope and the counteracting forces that are resistant to motion. Within this general framework, this work tests two hypotheses: (i) although conceptually and methodological distinct, the statistic and deterministic methods generate similar shallow slides susceptibility results regarding the model's predictive capacity and spatial agreement; and (ii) the combination of shallow slides susceptibility maps obtained with statistical and physically-based methods, for the same study area, generate a more reliable susceptibility model for shallow slides occurrence. These hypotheses were tested in a small test site (13.9 km^2) located north of Lisbon (Portugal) using a statistical method (the Information Value method) and a physically-based method (the Infinite Slope method). The landslide susceptibility maps produced with the statistic and deterministic methods were combined into a new landslide susceptibility map. The latter was based on a set of integration rules defined by the cross-tabulation of the susceptibility classes of both maps and analysis of the corresponding contingency tables. The results demonstrate a higher predictive capacity of the new shallow slides susceptibility map, which combines the independent results obtained with statistical and physically-based models. Moreover, the combination of the two models allowed the identification of areas where the results of the Information Value and the Infinite Slope methods are contradictory. Thus, these areas were classified as uncertain and deserve additional investigation at a more detailed scale.

Keywords: Shallow slides, susceptibility, Information Value, Infinite Slope, Factor of Safety, models combination.

1 Introduction

The evaluation of landslide susceptibility has been carried out worldwide based on three fundamental principles (Varnes et al., 1984; Carrara et al., 1991; Hutchinson, 1995; Guzzetti, 2005): (i) the landslides can be recognized, classified and mapped; (ii) the conditions that cause instability (predisposing factors) can be identified, registered and used to build predictive models; and (iii) the occurrence of landslides can be spatially inferred. Within this conceptual scheme, it is

assumed that future landslides are more likely to occur in areas where geologic and geomorphologic conditions are similar to those that originated the slope instability in the past (Guzzetti et al., 1999). This conceptual scheme has been extended to different methods of landslide susceptibility assessment regardless of their nature (Varnes et al., 1984; Hutchinson, 1995; Aleotti and Chowdhury, 1999; Carrara et al., 1999; Fell et al., 2008b). This is nonetheless surprising since the conceptual

5 model is perfectly applied to any statistical method used to assess landslide susceptibility, but the same is not true for the physically-based methods. Indeed, the latter methods are based on physical laws and soil mechanics principles where the slope is considered as a system where shear stress and shear strength are continually in opposition. Unlike landslide susceptibility models based on statistical methods, landslide inventories are not used to assess landslide susceptibility with deterministic methods. However, landslide inventories still remain essential to validate the obtained landslide susceptibility

10 maps. In addition, landslide inventory information is frequently used for calibrating stability models through back-calculation (e.g., Delmonaco et al., 2003; Teixeira et al., 2015).

The comparison between different methods to assess landslide susceptibility is not a new research topic when performed exclusively with different statistical methods (Gorsevski et al., 2003; Süzen and Doyuran, 2004; Brenning, 2005; Davis et al., 2006; Lee et al., 2007; Felicísimo et al., 2013; Bui et al., 2016) or with different physically-based methods (Zizioli et al.,

15 2013; Formetta et al., 2014; Pradham and Kim, 2015; Teixeira et al., 2015). There are a few studies that compare the predictive capacity between statistical and physically-based methods (Crosta et al., 2006; Carrara et al., 2008; Frattini et al., 2008; Yilmaz and Keskin, 2009; Cervi et al., 2010; Goetz et al., 2011; Seefelder et al., 2016) and out of those only a limited number have combined the results obtained with statistical and physically-based approaches (Chang and Chiang, 2009; Günther and Thiel, 2009; Goetz et al., 2011). According to Zizioli et al. (2013) the different methods used to assess shallow

20 slides susceptibility are not mutually exclusive. The latter authors pointed out that the use of different strategies to assess landslide susceptibility and the comparison of their predictive capacity can help to: (i) enhance the quality and reliability of each method; (ii) highlight and identify the most important factors affecting the slope instability system; (iii) neglect less influential aspects to simplify the models; and (iv) select the most appropriate methodology to achieve a specified goal.

In the present study, the basin scale refers to the river basin limits (e.g. Guzzetti et al., 2005; Remondo et al., 2005). The

25 relevance for using this study area limits when assessing rainfall-triggered landslides susceptibility is related with the maintenance of the hydrologic processes continuity, mainly runoff and potential infiltration. In addition, the basin scale is adjusted to the susceptibility zonation recommendations proposed for modelling scales between 1: 25,000 and 1:5,000 (Cascini, 2008; Fell et al., 2008b) and for study areas ranging in size from 10 to 1000 km^2 (Fell et al., 2008b).

In this study we test two hypotheses: (i) although conceptually and methodologically distinct, the statistic and deterministic

30 methods generate similar results for shallow landslides susceptibility regarding the model's predictive capacity and spatial agreement; and (ii) the combination of the shallow landslides susceptibility maps obtained with statistical and physically-based methods, for the same study area, generate a more reliable susceptibility map for shallow slides occurrence.

2 Study area

The study area comprises the two small catchments of Monfalim and Louriceira (13.9 km^2), which are located 25 km NNW of Lisbon, Portugal (Fig. 1). The elevation ranges from 442 m at the West to 134 m in the northeast sector of the study area, near the confluence of both Monfalim and Louriceira rivers with the Grande da Pipa River (GPR), which is an affluent of the Tagus River.

The lithological units are mainly sedimentary rocks dated from the Kimmeridgian to the Lower Thitonian (Upper Jurassic). There are also alluvium deposits of the Holocene age and a complex of dikes and volcanic masses that cover only 1.1 % of the study area. The detailed lithological units map of the study area (Fig. 1) was constructed based on official geological maps (Zbyszewski and Assunção, 1965; INETI, 2005) and on the interpretation of aerial photographs and validation of lithological units limits through field work. Therefore, it was possible to identify the following eight lithological units (from L1 to L8): (L1) alluvium; (L2) limestones and marls; (L3) sandstones and limestones; (L4) mudstones and marly limestones; (L5) limestones; (L6) marls; (L7) mudstones and marls; and (LU8) dykes and volcanic masses (basalt, teschenite and dolerite).

The study area has undergone a general tectonic uplift since the Miocene (Zbyszewski and Assunção, 1965) and the layers dip typically to SE/SW. This structural setting, together with the alternation of soft rocks such as marls, clays and mudstones with more resistant rocks as the limestones, has allowed the development of cuesta-like landforms resulting from differential erosional processes (Ferreira, 1984; Ferreira et al., 1987; Zêzere, 1991). The slopes within the study area are typically moderate: 78.1 % of the total area has slopes in the range of 5º to 20º. The gentle slopes (0º – 5º) represent only 12.9 % and the steepest slopes (> 20º) occur only in 9 % of the study area.

Landslides in the study area have been triggered by rainfall (Zêzere et al., 1999, 2005, 2015; Zêzere and Rodrigues, 2002; Oliveira, 2012). The climate is Mediterranean and the Mean Annual Precipitation (MAP) is 730 mm (at São Julião do Tojal gauge located 20 km south from the study area) (Zêzere et al., 2015). Shallow slides have been triggered mainly by intense short duration rainfall episodes, of typically 1 to 15 days maximum (Zêzere and Trigo, 2011; Zêzere et al., 2015). These rainfall events generate increments of pore water pressures and the reduction of the soil shear strength, including the loss of cohesion on fine sediments, which promote the failure along the superficial soil formations or along the contact between the soil and the impermeable bedrock (Trigo et al., 2005).

3 Methods and data

The methodological procedures for assessing shallow slides susceptibility based on the application and combination of statistical and physically-based approaches are summarized in Fig. 2. Two commonly used methods were chosen: the bivariate statistical Information Value method (IV) (Yin and Yan, 1988) and the Infinite Slope method (IS) (Sharma, 2002) based on the calculation of the Factor of Safety (FS). Both methods are in line with the experts panel recommendations to assess landslide susceptibility (Cascini, 2008; Fell et al., 2008a, 2008b; Corominas et al., 2014) and have been applied

successfully in similar geological and geomorphological context in the region north of Lisbon (Zêzere, 2002; Pimenta, 2011; Guillard and Zêzere, 2012; Oliveira et al., 2015).In order to model the shallow slides susceptibility, the dependent variables (shallow slides training and validation groups), the independent dataset of variables used as predisposing factors, and the maps representing geotechnical and hydraulic parameters were rasterized using a pixel of 5 m x 5 m.

5 3.1 Landslide inventory

The landslide inventory was used twice in this study: (i) to establish the statistical relationships between shallow slides and the data-set of environmental factors assumed as shallow slides predisposing factors in the statistical approach; and (ii) to validate the shallow slides susceptibility models obtained with both statistical and physically-based models. The landslide inventory of the study area (Fig.1) includes 111 shallow slides (translational and rotational slides with high curvature angle
10 of the slip surface) that were classified following the Cruden and Varnes (1996) proposal. The depth of the slip surface is typically less than 1.5 m and, as a rule, the shear planes are located in the interface between the soil coverture and the bedrock. The mean landslide area and volume are, respectively, 513 m^2 and 573 m^3 (Table 1). The shallow slides inventory was extracted from (Oliveira, 2012) and was based on the interpretation of aerial photographs (1983, 1989) and orthophotomaps (2003, 2004, 2007), as well as on extensive field work carried out during the 2006-2010 period.
15 The inventory of shallow slides was further subjected to a partition based on a temporal criterion (Fig.1, Table 1). Table 1 summarizes the mean shallow slide characteristics considering the total inventory and two sub-sets (training group and validation group) for the entire study area. The landslide training group includes the shallow slides that occurred until the end of 1983 (51 cases, 0.027 km^2, and 0.19 % of the study area). The landslide validation group includes the shallow slides that occurred between 1984 and the end of 2010 (60 cases, 0.03 km^2, and 0.22 % of the study area). The training group was
20 used to weigh classes of shallow slides predisposing factors in the statistical model using the IV method, and it was also used to calibrate the shear strength parameters (cohesion and friction angle) of the lithological units in the IS model. The validation group was used for the independent validation of both statistical and physically-based shallow slides susceptibility models. The shallow slides density, area and volume occurred in each lithological unit are summarized in Table 1. The larger shallow slides are observed within lithological units L2 and L4 where the landslides area and volume are above the mean.
25 Smaller shallow slides are observed within lithological units L3, L5, L7 and L8, where area and volume of landslides are below the mean (Table 1).

3.2 Statistical approach to assess landslide susceptibility

3.2.1. The Information Value method

The Information Value (IV) (Yin and Yan, 1988) was used to compute the susceptibility score for each class of each variable
30 considered as a landslide predisposing factor based on the log normalization of the ratio between the conditional probability

to find a shallow slide in a certain class of a predisposing factor and the a priori probability to find a shallow slide in the study area, following Eq. (1).

$$Ii = log \frac{Si/Ni}{S/N} \ , \tag{1}$$

where: Ii is the Information Value of class Xi belonging to an independent variable (landslide predisposing factor); Si is the number of pixels with shallow slides belonging to the training group and the presence of the variable class Xi; Ni is the number of pixels with variable class Xi; S is the total number pixels with shallow slides belonging to the training group; and N is the total number of pixels of the study area. Due to the logarithmic normalization Ii cannot be calculated when no

10   shallow slides are registered in a certain predisposing factor class ($Si = 0$). In these cases the Ii was forced to be equal to the millesimal value lower than the lowest Ii within the predisposing factor. The final IV scores Ij for each terrain unit j was obtained using Eq. (2).

$$Ij = \ \sum_{i=1}^{m} Xij \ Ii \ , \tag{2}$$

where: m is the total number of variable classes; and Xij is either zero if the variable class is not present in the pixel j, or one if the variable class is present.

3.2.2 Landslide predisposing factors

We selected the following seven landslide predisposing factors as independent variables (Fig. 1, Fig. 3 and Table 2 for the

20   description of classes) that have successfully been used in previous studies in the region north of Lisbon (e.g., Oliveira et al., 2015): lithology, slope angle, slope aspect, slope curvature, topographic position index (TPI), slope over area ratio and land use.

The lithologic map includes eight classes described above (cf. Sect. 2. Study area). The Land use map was obtained from the official map representing the land use in 1990. Although it does not match the current land use in the study area, it is the one

25   that best fits the time span of shallow landslides included in the present landslide inventory and the temporal land use frame closer to the age of the landslides in the training group. The remaining variables (slope, aspect, curvature, topographic position index and slope over area ratio) were derived from a Digital Elevation Model based on elevation data interpolated from a topographic contours map (equidistance 10 m). Regarding the curvature map, a DEM generalization based on a 50 m pixel size grid was considered to calculate the profile of the slopes, as it provides the best fit to the morphology of slopes in

30   the study area (Oliveira et al., 2015). The Topographic Position Index (TPI) was calculated based on the Facet Corridor Designer tool for ArcGIS and compares the elevation value of each cell in the DEM with the mean elevation value of the neighbouring cells, at a given maximum distance (Jenness et al., 2011). This index is heavily dependent on the scale

(Piacentini et al., 2015) an the neighbourhood radius of 25 meters proved to be the most appropriate for the index calculation at the work reference scale. The Slope Over Area Ratio (SOAR) was used to express the importance of the topography in hydrological processes through the relationship between the slope and the contribution area (Sørensen et al., 2006), which allow to infer the areas prone to surface saturation (Fonseca, 2005). The calculation of the SOAR was made using the TauDEM 5.2 (Terrain Analysis Using Digital Elevation Models) tool and the algorithm D8 (O'Callagham and Mark, 1984) to minimize the dispersion of accumulation flow.

3.3 Physically-based approach to assess landslide susceptibility

3.3.1 The Infinite Slope method (IS)

The most popular formulations of the Infinite Slope method consider a subsurface flow/water table level parallel to the topographic surface, whose maximum depth is equivalent to the maximum thickness of the saturated soil. In this context, the development of a steady-state hydraulic model in static conditions can be related to the ratio between the thickness of saturated soil and the thickness of the potentially unstable soil, as provided in the formulation of SHALSTAB model (Dietrich and Montegomery, 1998). The FS for each terrain unit (pixel) was thus calculated based on the Infinite Slope method, incorporating a soil thickness model and an hydraulic model for the study area, following Eq. (3) (Sharma, 2002):

$$FS = \frac{c' + h * \cos^2\beta [(1-m)Y_m + m\, Y_{sub}] * \tan\phi'}{h * \sin\beta * \cos\beta [(1-m)Y_m + m\, Y_{sat})} , \tag{3}$$

Where: c' is the effective cohesion (kN/m²); h is the potentially unstable soil depth; β is the slope of the terrain unit; m is the equation component of the hydraulic model, considered as the ratio between the saturated soil depth and the potentially unstable soil depth; ϕ' is the internal friction angle (°); γ_m is the specific soil weight (kN/m³); γ_{sat} is the saturated soil weight (kN/m³) and γ_{sub} is the submerged soil weight (kN/m³). The FS values can be interpreted in two ways. In the more restrict sense it is assumed that all terrain units with FS values ≤ 1 are unstable. In a broader interpretation the FS results are compared with results obtained using the statistical approach; in other words each terrain unit within a study area can be ranked according to its FS value, where the lowest FS value indicates the highest landslide susceptibility.

The development of the IS model was supported by the following parameters: (i) topographical variables (slope and catchment area), (ii) soil thickness, (iii) hydrologic parameters (hydraulic conductivity, soil transmissivity and daily rainfall threshold), (iv) geotechnical parameters (natural, saturated and submerged specific soil weights; cohesion; and internal friction angle). Most geotechnical parameters were deduced from references with regional validity that were summarized by (Pimenta, 2011).

3.3.2 Soil thickness model

The depth of the potentially unstable soil is a critical parameter that strongly influences the stability of slopes. The soil depth model for the study area was obtained using Eq. (4), as proposed by (Catani et al., 2010):

5   $h = -K_c . C . \eta . \Psi^{-1}$,   (4)

Where: h is the soil thickness, K_c is a constant calibration parameter, C is an index based on the slope profile curvature, η is the relative soil depth dependent on the topographic position; ψ^{-1} is the critical slope angle associated to landslide occurrence. The three parameters C, η and ψ^{-1} were expressed in a scale ranging between zero and one. For each parameter,

10 the value one was assigned to the maximum observed value, zero to the minimum observed value and the remaining observed values were assigned numbers between zero and one by linear normalization. The constant K_c was estimated independently for each lithological unit based on trial and error estimation to obtain the best possible fit of the soil thickness values obtained by Eq. 4 to the soil thickness values measured in 110 sampling field points. These sampling field measurements, subject to the existence of slope cuts where the soil depth was measured, were spatial distributed in order to

15 guarantee a reasonable number of soil thickness measurements in each lithological unit but also along different geomorphological units (interfluve areas, slopes, valley floors) The calibration of the K_c constant for any lithological unit requires that the differences between the maximum estimated soil thickness and the maximum soil thickness measured in the field does not exceed one meter. Table 3 summarizes the K_c constant calibration values obtained for each lithological unit (from L1 to L8) in the study area. Soil profiles were not found in lithological units L1, L3 and L8 during the field work. In

20 the case of lithological unit L3, we adopted a K_c value equal to the one estimated for the other lithologic unit of the same age (L4, $K_c = 3.6$). In the case of alluvium (L1) and complex of dikes and masses (L9) we adopted a $K_c = 2.9$, which is the arithmetic mean of all K_c values obtained for lithological units where it was possible to measure soil thickness during field sampling. Fig. 4A shows the final soil thickness map of the study area and Fig. 4B shows the correlation between the soil thicknesses measured in the field and the soil thicknesses values extracted from the final soil thickness model (Fig. 4A).

25 Although the constrain of the soil thickness model to a one meter-error maximum between the estimated and field measured soil thickness, this condition was only possible to assign to 102 sampling field points (Fig. 4B). For these cases a coefficient of determination of 0.62 was obtained. Nevertheless, for eight sampling field points (7.3 % of total) the observed error was higher than one meter, ranging from 1.1 and 2.1 m.

3.3.3 Hydraulic model

The adopted hydraulic model was developed using SHALSTAB (Dietrich and Montegomery, 1998), that follows a model developed by O' Loughlin (1986). According to Sharma (2002), the hydraulic model is the ratio between the thickness of saturated soil and the thickness of the potentially unstable soil given by Eq. (5).

$$\frac{h}{z} = \frac{Q}{T} * \frac{a}{b*Sin\beta} ,$$ (5)

Where: h/z is the ratio between the thickness of the saturated soil above the impermeable layer and the thickness of the potentially unstable soil; Q is the effective precipitation (m/day); T is the transmissivity of the soil (m²/day); a is the

10 upstream contribution area (m^2); b is the cell length (m); and β is the slope gradient (°). The increase of the hydrologic ratio (Q/T) indicates that soil saturation will be faster and more extensive. The topographic ratio ($a/(b * Sin\beta)$) describes the topography effect on runoff (Dietrich and Montegomery, 1998; Montgomery et al., 1998). The transmissivity of the soil was estimated using Eq. (6) (Lencastre and Franco, 2006):

15 $$T = k + z ,$$ (6)

Where: T is the soil transmissivity (m²/day); k is the saturated hydraulic conductivity (m/day); and z is the soil thickness (m). As the hydraulic conductivity based on field measurements was not available for the study area, this parameter was estimated for the identified soil types based on the work developed by Rawls et al. (1982), which summarized the typical

20 hydraulic conductivities for different soil types starting from the respective textural properties. The national digital soil map at 1: 25,000 scale (DGADR, 1999) was used to extract the clay, silt + sand, and coarse sand fractions for the different soils types in the study area. The soil taxonomy of the US Department of Agriculture was used to distinguish between soil types, through the Soil Texture Triangle Bulk Density. Rocky outcrops and urban areas were assigned the value -1 value, thus corresponding to zero (absence of water) in the hydraulic model. The castanozems soils were also assigned the value -1

25 value because the typical pedological stage of castanozem soils within the study area is a stony soil phase. Finally, 55 types of soils were identified, in addition to social areas and rocky outcrops.

The effective precipitation was estimated based on the Eq. (7) proposed by Trigo et al. (2005) that defines the rainfall threshold for triggering translational and rotational landslides in the region north of Lisbon that includes the study area.

30 $$Cr = 7.4D + 107 ,$$ (7)

Where: Cr is the rainfall threshold that is associated to landslides occurrence (mm), and D is the number of consecutive rainfall days.

As most landslide events occur in the study area during the Winter season we believe that the effect of evapotranspiration can be neglected; therefore the effective precipitation can be assumed to equal the total precipitation, namely for short rainfall periods. Using Eq. (7) we obtained a critical daily rainfall for failure of 114.4 mm. The rainfall concentrated in a single day is a feasible scenario for triggering shallow landslide events, such as the ones that occurred in the Lisbon Region in 1967 and 1983 (Zêzere et al., 2005, 2015).

The hydraulic conductivity was estimated based on the critical precipitation for failure and the soil texture. In the study area k ranges from 5.05 m/day in the luvisols with dominantly sandy texture, to 0.0144 m/day in vertisols with dominantly clayey texture. The computed transmissivity ranges between zero and 13.45 m^2/day (Fig. 5A). The final hydraulic model is shown in Fig. 5B.

3.3.4 Geotechnical parameters of superficial soils

All geotechnical parameters mentioned in this section, related to soil weight (Ym, $Ysat$, $Ysub$) cohesion (c') and friction angle (ϕ'), were based on literature and were defined specifically for the superficial soils above the bedrock within each lithological unit.

Superficial soils in the study area are mainly regoliths and colluvium deposits that had suffered little mobilization along the slopes, which is explained by the low energy of the existing landforms. As a consequence, soils above the bedrock are typically shallow and can be assumed to be very close to the parent lithology regarding composition. Therefore, in this case study, we consider appropriate to use the lithological mapping units for the regionalization of the shear strength parameters of the superficial soils above the bedrock. The specific (Y_m), saturated (Y_{sat}) and submerged (Y_{sub}) soil weights values were provided by Pimenta (2011) for the superficial soils above the bedrock within each lithological unit and are summarized in Table 4.

The strength parameters of the lithological units obtained in laboratory with direct shear tests Pimenta (2011) proved to be too high to explain the observed slope instability. Therefore, the optimal combinations of cohesion and effective internal friction angle values for each lithological unit were defined iteratively through back analysis. Different combinations of cohesion and effective internal friction angles were tested with the Infinite Slope method and validated with the landslide training group (landslide area), using as reference the maximum and minimum friction angles suggested by Geotechdata (2013). Critical pairs of cohesion and internal friction angle were selected for each lithological unit by combining two criteria: (i) the susceptibility class with FS ≤ 1 must include at least 50 % of landslide area of the landslide training group located on the lithological unit; and (ii) the susceptibility class with FS ≤ 1 must have the highest effective ratio, which is expressed by the ratio between the percentage of landslide area predicted in the class and the percentage of the class area in the study area (Chung and Fabbri, 2003). In the cases of lithological units L2 and L5 it was not possible to comply with the criterion (i), but the corresponding critical pair cohesion / internal friction angle were selected respecting criterion (ii). In addition, strength parameters of lithological units L1 and L8 could not be estimated with this method due to the absence of landslides in these lithological units. In these cases, the cohesion and effective internal friction angle were derived directly

from Pimenta (2011), that gathered information from technical reports, geotechnical laboratory tests and standard values reported in the literature (Baptista, 2004; Cernica, 1995; Fernandes, 1994; Jeremias, 2000; Vallejo et al., 2002). Table 4 summarizes the geotechnical parameters of the lithological units used to implement the physically-based model.

3.4. Validation, comparison and combination of shallow slides susceptibility models

5 The validation of susceptibility maps produced by statistical and physically-based models was made independently using the landslide validation group. ROC (Receiver Operating Characteristic) curves were computed and the corresponding Area Under the Curve (AUROC) was calculated. Additionally, the landslide susceptibility maps were classified and the effective ratio of each class was estimated. Both statistical and physically-based susceptibility maps were classified considering the same fraction of study area in each equivalent landslide susceptibility class. First, the IS map was ranked into five classes

10 based on the Factor of Safety values (≤ 1, 1 to 1.25; 1.25 to 1.5, 1.5 to 2, and > 2), which correspond respectively to the following descriptive classification of susceptibility (Very high; High; Moderate, Low; and Very low). Next, the IV map was organized into five classes (Very high; High; Moderate, Low; Very low) ensuring that equivalent susceptibility classes cover the same fraction of the study area in both maps. The evaluation of the spatial agreement between landslide susceptibility maps based on statistical and physically-based approaches was made using the Rank Difference Tool included in ArcSDM

15 (Sawatzky et al., 2008).

Lastly, statistical and physically-based susceptibility maps were combined into a final shallow slides susceptibility map based on the intersection of the susceptibility classes in a contingency table, using the Map Comparison Kit tool (Visser and Nijs, 2006) on a cell by cell comparison and Kappa statistics.

4 Results and discussion

20 **4.1 Statistical landslide susceptibility assessment**

The Information Value scores calculated for each class of predisposing factors based on the landslide training group are summarized in Table 2 and the corresponding shallow slides susceptibility map is shown in Fig. 6. The spatial distribution of susceptibility shows a clear contrast between the northern/north-eastern sectors of the study area in which the susceptibility is predominantly classified as low to very low, whereas in the central/southern part of the study area the susceptibility to

25 shallow slides is typically higher. This contrast is mainly justified by the lithological differentiation. In fact the lithological units L7 (marls and clays) and L5 (limestones) are found in the northern part of the study area, and they apparently have a low predisposition to shallow slide occurrence (Table 2). By opposition, lithological units more prone to slope instability (L2, limestones and marls; and L3, sandstones and limestones) occur as outcrops in the central and southern part of the study area. In addition, the slope angle tends to be higher in the latter part of the study area, thus contributing to the higher

30 landslide susceptibility.

The ROC curve of the landslide susceptibility model is shown in Fig. 7. The IV model predictive capacity is reasonable/good, as expressed by the AUROC of 0.75.

4.2 Physically based landslide susceptibility assessment

The shallow slides susceptibility map computed with the IS method is shown in Fig. 8A. The susceptibility class with FS ≤1
5 (Very high susceptibility) covers 17.9 % of the total study area and validates 53.4 % of the shallow slides belonging to the landslide validation group, which explains the higher effective ratio (2.98) of this susceptibility class (Table 5). By comparison with the IV susceptibility map the increment of area classified with very high/high susceptibility is clear in the northern sector of the study area where lithological unit L7 outcrops, whereas the spatial expression of the two highest landslide susceptibility classes decreases in the southwestern/southern sector where the lithological unit L2 outcrops. The
10 ROC curve of the model based on the landslide validation group is shown in Fig. 7. The ROC curve is closer to the upper left corner of the ROC curve graphic, which confirms the best predictive capacity of the IS susceptibility map when compared with the IV susceptibility map. The AUROC of 0.81 also supports the better predictive capacity of the IS model.

As mentioned above, shallow landslides have been triggered by rainfall in the study area, typically during intense short duration rainfall events (Zêzere et al., 2005, 2015; Zêzere and Trigo, 2011). Additionally, extensive field work in the study
15 area (Oliveira, 2012) has shown a total absence of instability signs during the summer, which is consistent with the dryness that characterizes this season. Therefore, a typical situation of superficial absence of water in the soil during summer, i.e., m = 0, is implicit; accordingly, an additional physically-based shallow slides susceptibility map was prepared considering no water in the soil (m = 0). Figure 8B shows the model results. Given the assumed boundary conditions, it was expected that the model would not generate FS ≤ 1. However, Fig. 8B shows a small fraction of the study area classified with Very high
20 susceptibility (FS ≤ 1, 2.25 % of study area) under conditions of absence of water into the soil, which is interpreted as an error of the IS model. It is worth mentioning that most of the model errors occur over the lithological unit L2 indicating that the corresponding resistance parameters (cohesion, internal friction angle) may be underestimated.

The cohesion and internal friction angle values that guarantee FS>1 for any lithological unit in the absence of water into the soil (m = 0) are summarized in Table 4 (in brackets). These geotechnical parameters were tested in a new model considering
25 the existence of water into the soil (susceptibility map not shown in the present work) and the obtained result is not reliable: the area classified as unstable (with FS ≤ 1) corresponds to only 1.3% of the total study area and validates only 8.1% of the landslides belonging to the training group. Therefore, we conclude that the geotechnical parameters that guarantee the absence of cells with FS ≤1 when m = 0 (features in brackets in Table 4) are too high to correctly express the landslide susceptibility in the study area.

4.3 Comparison of landslide susceptibility models

The comparison of the susceptibility maps produced with IV and IS methods demonstrates that spatially the susceptibility ranking differs substantially depending on the method used. Indeed, the Kappa coefficient is only 0.23, which means that spatial correlation is moderate, although the reasonable/good predictive capacity of both models was attested by the AUROC (Fig.7).

Table 5 summarizes the spatial extension, the percentage of shallow slides of the landslide validation group and the effective ratio of each susceptibility class for the two predictive models (IV and IS). The two highest classes in the IV landslide susceptibility map spread over 34.1 % of the total study area and the corresponding percentage of predicted shallow slides approaches 69.4 %. The performance of the predictive model is weaker for the intermediate susceptibility classes (moderate and low), in particular for the low susceptibility class that includes a relevant portion (15.7 %) of shallow slides belonging to the landslide validation group. The IS landslide susceptibility model reveals a better predictive capacity confirmed by the fact that 83.1 % of the landslide validation group fall into the two highest susceptibility classes.

The effective ratios calculated for landslide susceptibility classes of both models are summarized in Table 5. The effective ratios for the IS model are higher for the Very high and High susceptibility classes and lower for the Low and Very low susceptibility classes than the effective ratios of the IV model for the same classes, which indicate a better predictive capacity of the IS model.

The spatial comparison of the two susceptibility maps is shown in Fig. 9. The value zero means spatial agreement between landslide susceptibility classes, whereas values other than zero mean disagreement. Negative values indicate that landslide susceptibility obtained with IV is lower when compared with the map obtained with IS, with the difference increasing from -1 to -4. For example, a grid cell with a score -4 means this terrain unit was classified as very high susceptibility in the IS susceptibility map and as very low susceptibility in the IV susceptibility map. Positive values indicate the opposite relationship between map classes. The perfect spatial agreement between susceptibility classes in both maps occurs in 39.9 % of the study area (Table 6). However, adding the minimum mismatch classification (-1 and +1 in Fig. 9) the previous feature rises to 73 % of the total study area. The major discrepancy between the two susceptibility maps (-4, -3, 3 and 4 in Fig. 9) occurs along 10.5 % of the study area, namely where the lithological units L7 and L2 outcrop. In the northern part of the study area where the lithological unit L7 is present, the landslide susceptibility obtained with the IV method is lower than the one obtained with the IS method, whereas the opposite occurs in the central and southern part of the study area where the lithological unit L2 is present.

These results can be explained by the particular specifications associated with the physically-based and statistical methods. The resistance parameters estimated for the superficial soil over lithological unit L7 ($c' = 2$ kPa, $\varphi' = 19$ °) are higher than those estimated for lithological unit L2 ($c' = 0.5$ kPa $\varphi' = 17$ °). However, the landslide susceptibility computed using the IS tends to be higher over lithological unit L7, which is related to the soil water content and eventually to the presence of thicker soils, particularly along the lower part of slopes where topographic conditions are more prone to soil

saturation. On the other hand, the statistical approach generated IV scores of 0.494 and -0.857, respectively for lithological units L2 and L7. The positive IV score for lithological unit L2 clearly indicates a higher likelihood of shallow slides occurrence. We acknowledge that shallow slides inventory may be incomplete in the area corresponding to lithological unit L7, which could justify the negative IV score. The slope and land use clusters observed within lithological units L2 and L7 are shown in Fig. 10A and 10B. The lithological unit L7 (clays and marls) are mainly associated with gentle and moderate slopes (slope angles between 5 to 15º) and are characterized by intense agricultural use that extends over 78.1 % of the L7 surface; thus, the footprint of small shallow slides is easily erased on the landscape, as the "original" slope profile is recovered for agricultural activities. On the contrary, the lithological unit L2 is constituted by sequences of marl and limestone layers, which induce larger topographic irregularities and less productive soils on steep to moderate slopes. The existing geological and geomorphological conditions favoured the prevalence of forest and annual crop cultures besides the intensive agricultural activity. In this context, the landslide footprint over slopes tends to last longer, as proven by the larger number of shallow slides mapped over lithological unit L2 (Table 1: 45 shallow slides, 8.3 shallow slides/km^2) when compared with lithological unit L7 (Table 1: 17 shallow slides, 5.2 landslides/km^2). Therefore, the inventory of shallow slides is assumed to be more complete over lithological unit L2, which explains the higher IV score.

4.4. Combination of landslide susceptibility models

The results of the cross-tabulation between landslide susceptibility classes of both susceptibility maps (statistical and physically-based) are summarized in a contingency table (Table 6). The distribution of shallow slides belonging to the validation group on the same contingency table is summarized in Table 7. Table 6 shows the combinations considered within the contingency table to classify the final landslide susceptibility map resulting from the integration of statistical and physically-based predictive models; the colours (red, orange, yellow, light green, green and grey) represent the final susceptibility classes (Very high, High, Moderate, Low, Very low, and uncertain, respectively). The corresponding final shallow slides susceptibility map is shown in Fig. 11 and information about final landslide susceptibility classes is detailed in Table 8.

The Very high susceptibility class covers 16.4 % of the study area and includes 55.6 % of the shallow slides validation group and the High susceptibility class covers 14.3 % of the study area and includes 18.6 % of the shallow slides. In opposition, the Very low and Low susceptibility classes cover 33.4 % and 10.6 % of the study area, respectively, and include only a small fraction of the landslide validation group (1.4 % each class).

Terrain units classified as Very high or High susceptibility by one method and simultaneously as Very low or Low susceptibility by the other method were considered as uncertain regarding susceptibility to shallow slides occurrence in the final map. The 'grey' class, although classified as Uncertain, is potentially High or Very high landslide susceptible and covers 16.3 % of the study area and includes 16.0 % of the shallow slides belonging to the validation group. However, the distribution of landslide validation group in the Uncertain susceptibility class is different in the upper right corner and in the

lower left corner of the contingency table (see Tables 6 and 7). Terrain units classified as Very high or High susceptibility by the IS susceptibility map and as Very low or Low susceptibility by the VI method (upper right corner in Tables 6 and 7) include 14.7 % of shallow slides belonging to the validation group, whereas terrain units with inverse classification (lower left corner in Tables 6 and 7) only contain 1.2 % of the shallow slides validation group. These values, once more, reflect the

5   higher quality of the physically-based susceptibility model in comparison with the statistical model.

The predictive quality of susceptibility classes that make up the final landslide susceptibility map is confirmed by the estimated effective ratios (Table 8). The effective ratio of the Very high susceptibility class (3.39) is higher than those obtained for the equivalent susceptibility class with the statistical and physically-based methods (cf. Table 5). In addition, effective ratios corresponding to the Very low and Low susceptibility classes (0.04 and 0.12, respectively) are lower than

10   those obtained with statistical and physically-based methods (cf. Table 5), which indicates a better predictive performance of the combination of the two landslide susceptibility models. Moreover, the effective ratio is higher for the Uncertain class than for the Moderate class (Table 8), which is consistent with the potential for high or very high susceptibility considered for the Uncertain class.

5 Conclusion

15   Statistical and physically-based methods used to assess landslide susceptibility at the basin scale are conceptually distinct as the former are based on weighing environment predisposing factors, whereas the latter are supported by the computation of shearing and resistance forces along potential slip surfaces. The existence of a landslide inventory is crucial to weigh predictive variables within statistical methods, which is not the case of physically-based methods that can be computed independently on the landslide inventory. Both types of methods have advantages and drawbacks. The major

20   constrains associated to statistical approaches have been summarized in previous works (Corominas et al., 2014; Fell et al., 2008a) and result from: (i) the difficulty of establishing causal (cause-effect) relationships between variables; (ii) problems arising from self-correlation between variables; (iii) the typically not normal statistical distribution of predictor variables; (iv) the limitations related to the quality of data, in particular the completion of the landslide inventory; and (v) the difficulty in transferring the results from the study area to other areas, even with similar characteristics. In the case of physically-based

25   methods, the major constrains were listed as follow (Corominas et al., 2014; Fell et al., 2008a): (i) the high level of generalization and/or simplification regarding the spatial distribution of geotechnical or hydrological parameters; (ii) the feasibility of model application is limited to areas with relatively homogeneous ground conditions (e.g., geology and geomorphology); (iii) the uncertainties about the depth of the soil and of the slip surface; and (iv) the difficulties in predicting groundwater pore pressures and their relationship with rainfall.

30   In this work we tested two hypotheses: (i) although conceptually distinct, statistical and physically-based methods generate similar results concerning susceptibility to shallow slide occurrence; and (ii) a reliable landslide susceptibility map can be obtained for a single study area by combining two landslide susceptibility models (statistical vs physically-based).

To achieve the proposed objectives the Information Value method and the Infinite Slope method were chosen to build two landslide susceptibility maps. A shallow slides inventory was separated into two independent landslide groups adopting a temporal criterion. Although some differences exist regarding the morphometric characteristics and the spatial distribution over lithological units of the two shallow slides subsets (training group and validation group), they were used independently in order to allow model comparison and validation. The training group was used twofold to define the statistical relationships between landslides and the dataset of variables assumed as landslide predisposing factors by the IV method, and to calibrate the resistance parameters (cohesion and internal friction angle) within the IS method. The landslide validation group was used to validate both susceptibility maps independently.

Some sources of bias were identified in the present work. Firstly, although the infinite slope stability model remains physically-based, the used geotechnical parameters lose, to some extent, their direct physical meaning since critical cohesion and internal friction angle combination were determined statistically assuming the highest effective ratio. Another potential source of bias is the use of the lithological map instead of the soil map to generalize the geotechnical properties of superficial soils. We acknowledge that the use of the soil map could be appropriate for that purpose taking in account the shallow characteristic of landslides. However, the national soil map at the 1:25,000 scale, provides 55 different soil type classes for the study area, which is a very large number to be balanced with the 51 shallow slides of the landslide training group used to evaluate the critical cohesion and internal friction angle parameters by back analysis. If landsides were regularly distributed over soil types, we would get only 0.9 shallow slides in each soil class, which is insufficient to estimate the resistance parameters. Moreover the occurrence of shallow slides was only verified on 18 of the 55 soil type classes, which would strongly increment the uncertainty of the regionalization of shear strength parameters based on the soil map.

When analysed separately, both methods generated good predictive results, although the physically-based model revealed to be more effective in the spatial prediction of shallow landslides, which is attested by the AUROC and the effective ratio of landslide susceptibility classes. In addition, the application of the Kappa statistics showed that the overall spatial agreement between susceptibility classes of both maps is only moderate (K = 0.23), so the first hypothesis is only partially confirmed. The major differences were registered over two lithological units (L2 and L7) and may result from the probable incompleteness of the shallow slides inventory over the lithological unit L7, as a consequence of human interventions related to agriculture activities.

Although similar approaches in the past merged mathematically the results obtained from two conceptually different susceptibility models (Günther and Thiel, 2009), in our work the final shallow slides susceptibility map was produced by combining the results obtained with the statistical and physically-based methods through a contingency table. The final result proved to be reliable, as shown by the effective ratio of the extreme susceptibility classes (Very high, Low and Very low). Thus, the second hypothesis is confirmed. Although it was possible to identify uncertain areas with one single model by varying some input assumptions and parameter combinations, our work demonstrates that the combination of both methods using a contingency table allowed the identification of areas classified as uncertain regarding landslide susceptibility but with potential to be highly/very highly susceptible to shallow slides occurrence, which is not possible when using a single

landslide susceptibility model. This is particular relevant in areas where the completeness degree of the landslide inventory is not equivalent over different lithological units, as is the case of the present study.

In future works an important contribute for augmenting the reliability of statistical models is the update of landslide inventory immediately after any landslide event, particularly in areas subject to intensive agricultural practice. The physical based models will certainly improve with a more reliable soil thickness model resulting from the densification of field soil sampling measurements covering all lithological and soil classes. The comprehensive aggregation of soil classes should sustain the more reliable regionalization of hydrological properties and shear strength parameters. In addition, the improvement of the resolution of the DEM of the study area using Lidar technology should increment the reliability of both landside susceptibility maps based on statistical and physically-based methods.

Author contribution

S. C. Oliveira and J. L. Zêzere conceptualized this study and supervised the complete work. S. C. Oliveira performed field work for landslide inventory and prepared the manuscript with contributions from all co-authors. S. Lajas, J. L. Zêzere and S.C. Oliveira performed field work for soil thickness measurement. S. Lajas prepared the cartographical and statistical input data for statistical and physically-based susceptibility modelling and validation. R. Melo contributes to the development of the soil thickness model, and to the estimation of geotechnical and hydrological parameters.

Ackonwledgements

This work was supported by the project FORLAND – Hydrogeomorphologic risk in Portugal: driving forces and application for land use planning (PTDC/ATPGEO/1660/2014) funded by Fundação para a Ciência e a Tecnologia, Portugal (FCT). Sérgio C. Oliveira has a postdoctoral grant (SFRH/BPD/85827/2012) funded by the Portuguese Foundation for Science and Technology (FCT). We are grateful to Martin Mergili, an anonymous reviewer and the Editor Andreas Günther, whose comments and suggestions helped to improve this work.

References

Aleotti, P. and Chowdhury, R.: Landslide hazard assessment: summary review and new perspectives, Bull. Eng. Geol. Environ., 58(1), 21–44, doi:10.1007/s100640050066, 1999.

Baptista, V.: Estudo das condições geológico-geotécnicas ocorrentes ao longo do sub-lanço Arruda dos Vinhos / Carregado da auto-estrada A10, Lisboa., 2004.

Brenning, A.: Spatial prediction models for landslide hazards: review, comparison and evaluation, Nat. Hazards Earth Syst. Sci., 5, 853–862, doi:10.5194/nhess-5-853-2005, 2005.

Bui, D. T., Tuan, T. A., Klempe, H., Pradhan, B. and Revhaug, I.: Spatial prediction models for shallow landslide hazards: a comparative assessment of the efficacy of support vector machines, artificial neural networks, kernel logistic regression, and logistic model tree, Landslides, 13(2), 361–378, doi:10.1007/s10346-015-0557-6, 2016.

Carrara, A., Cardinali, M., Detti, R., Guzzetti, F., Pasqui, V. and Reichenbach, P.: GIS techniques and statistical models in evaluating landslide hazard, Earth Surf. Process. Landforms, 16(5), 427–445, 1991.

Carrara, A., Guzzetti, F., Cardinali, M. and Reichenbach, P.: Use of GIS technology in the prediction and monitoring of landslide hazard, Nat. Hazards, 20, 117–135, doi:10.1023/A:1008097111310, 1999.

Carrara, A., Crosta, G. and Frattini, P.: Comparing models of debris-flow susceptibility in the alpine environment, Geomorphology, 94, 353–378, doi:10.1016/j.geomorph.2006.10.033, 2008.

Cascini, L.: Applicability of landslide susceptibility and hazard zoning at different scales, Eng. Geol., 102(3–4), 164–177, doi:10.1016/j.enggeo.2008.03.016, 2008.

Cascini, L., Ciurleo, M., Di Nocera, S. and Gullà, G.: A new-old approach for shallow landslide analysis and susceptibility zoning in fine-grained weathered soils of southern Italy, Geomorphology, 241, 371–381, doi:10.1016/j.geomorph.2015.04.017, 2015.

Catani, F., Segoni, S. and Falorni, G.: An empirical geomorphology based approach to the spatial prediction of soil thickness at catchment scale, Water Resorces Res., 46, 1–15, doi:10.1029/2008WR007450, 2010.

Cernica, J. N.: Geotechnical Engineering: Soil Mechanics, John Wiley & Sons, New York., 1995.

Cervi, F., Berti, M., Borgatti, L., Ronchetti, F., Manenti, F. and Corsini, A.: Comparing predictive capability of statistical and deterministic methods for landslide susceptibility mapping: A case study in the northern Apennines (Reggio Emilia Province, Italy), Landslides, 7(4), 433–444, doi:10.1007/s10346-010-0207-y, 2010.

Chang, K. and Chiang, S.: An integrated model for predicting rainfall-induced landslides, Geomorphology, 105(3–4), 366–373, doi:10.1016/j.geomorph.2008.10.012, 2009.

Chung, C.-J. F. and Fabbri, A. G.: Validation of spatial prediction models for landslide hazard mapping, Nat. Hazards, 65, 451–472, 2003.

Corominas, J., Westen, C. Van, Frattini, P., Cascini, L., Malet, J.-P., Fotopoulou, S., Catani, F., Eeckhaut, M. Van Den, Mavrouli, O., Agliardi, F., Pitilakis, K., Winter, M. G., Pastor, M., Ferlisi, S., Tofani, V., Herva, J. and Smith, J. T.: Recommendations for the quantitative analysis of landslide risk, Bull. Eng. Geol. Environ., 73, 209–263, doi:10.1007/s10064-013-0538-8, 2014.

Crosta, G., Carrara, A., Agliardi, F., Campedel, P. and Frattini, P.: Valutazione della pericolosità da caduta massi tramite un approccio integrato statistico e deterministico, G. di Geol. Appl., 4, 41–48, 2006.

Cruden, D. and Varnes, D.: Landslides types and processes, in Landslides investigation and mitigation, edited by A. Turner and R. Schuster, pp. 36–75, Transportation Research Board. National Academic Press, Washington DC., 1996.

Davis, J. C., Chung, C. J. and Ohlmacher, G. C.: Two models for evaluating landslide hazards, Comput. Geosci., 32(8), 1120–1127, doi:10.1016/j.cageo.2006.02.006, 2006.

Delmonaco, G., Leoni, G., Margottini, C., Puglisi, C. and Spizzichino, D.: Large scale debris-flow hazard assessment: a geotechnical approach and GIS modelling, Nat. Hazards Earth Syst. Sci., 3, 443–455, doi:10.5194/nhess-3-443-2003, 2003.

DGADR: Cartas dos Solos de Portugal - Cartas Complementares, , Folha 389, Escala 1:25000. SROA/CNROA/IEADR/IDRHA/, 1999.

5   Dietrich, W. and Montegomery, D.: SHALSTAB: A digital terrain model for mapping shallow landslide potential., 1998.

Felicísimo, Á., Cuartero, A., Remondo, J. and Quirós, E.: Mapping landslide susceptibility with logistic regression, multiple adaptive regression splines, classification and regression trees, and maximum entropy methods: A comparative study, Landslides, 10(2), 175–189, doi:10.1007/s10346-012-0320-1, 2013.

Fell, R., Corominas, J., Bonnard, C., Cascini, L., Leroi, E. and Savage, W. Z.: Commentary. Guidelines for landslide
10   susceptibility,   hazard   and   risk   zoning   for   land-use   planning,   Eng.   Geol.,   102(3–4),   99–111,
doi:10.1016/j.enggeo.2008.03.014, 2008a.

Fell, R., Corominas, J., Bonnard, C., Cascini, L., Leroi, E. and Savage, W. Z.: Guidelines for landslide susceptibility, hazard and risk zoning for land use planning, Eng. Geol., 102(3–4), 85–98, doi:10.1016/j.enggeo.2008.03.022, 2008b.

Fernandes, M. M.: Mecânica dos solos. Volume I, FEUP, Porto., 1994.

15   Ferreira, A.: Mouvements de terrain dans la region au nord de Lisbonne. Condition morphostructurales et climatiques, in Mouvements de terrain, pp. 485–494, Paris., 1984.

Ferreira, A., Zêzere, J. and Rodrigues, M.: Instabilite des versants dans la region au nord de Lisbonne. Essai de cartographie geomorphologique, Finisterra, XXII(44), 227–246, 1987.

Fonseca, I.: Modelling soil properties at the landscape scale in a desertification context, King's College London., 2005.

20   Formetta, G., Rago, V., Capparelli, G., Rigon, R., Muto, F. and Versace, P.: Integrated physically based system for modeling landslide susceptibility, Procedia Earth Planet. Sci., 9, 74–82, doi:10.1016/j.proeps.2014.06.006, 2014.

Frattini, P., Crosta, G., Carrara, A. and Agliardi, F.: Assessment of rockfall susceptibility by integrating statistical and physically-based approaches, Geomorphology, 94, 419–437, doi:10.1016/j.geomorph.2006.10.037, 2008.

Geotechdata: Angle friction. Mohr-Coulomb, [online] Available from: http://www.geotechdata.info/parameter/angle-of-
25   friction.html (Accessed 10 June 2015), 2013.

Goetz, J. N., Guthrie, R. H. and Brenning, A.: Geomorphology Integrating physical and empirical landslide susceptibility models using generalized additive models, Geomorphology, 129, 376–386, doi:10.1016/j.geomorph.2011.03.001, 2011.

Gorsevski, P. V., Gessler, P. E. and Jankowski, P.: Integrating a fuzzy k-means classification and a Bayesian approach for spatial prediction of landslide hazard, J. Geogr. Syst., 5(3), 223–251, doi:10.1007/s10109-003-0113-0, 2003.

30   Guillard, C. and Zezere, J.: Landslide Susceptibility Assessment and Validation in the Framework of Municipal Planning in Portugal : The Case of Loures Municipality, Environ. Manage., 50, 721–735, doi:10.1007/s00267-012-9921-7, 2012.

Günther, A. and Thiel, C.: Combined rock slope stability and shallow landslide susceptibility assessment of the Jasmund cliff area (Rügen Island, Germany), Nat. Hazards earth Syst. Sci., 9, 687–698, 2009.

Guzzetti, F.: Landslide hazard and risk assessment, Mathematisch-Naturwissenschaftlichen Fakultät der Rheinischen

Friedrich-Wilhelms-Universität University of Bonn,Bonn, Germany, defended on July 2006., 2005.

Guzzetti, F., Carrara, A., Cardinali, M. and Reichenbach, P.: Landslide hazard evaluation: A review of current techniques and their application in a multi-scale study, Central Italy, Geomorphology, 31(1–4), 181–216, doi:10.1016/S0169-555X(99)00078-1, 1999.

5   Guzzetti, F., Reichenbach, P., Cardinali, M., Galli, M. and Ardizzone, F.: Probabilistic landslide hazard assessment at the basin scale, Geomorphology, 72(1–4), 272–299, doi:10.1016/j.geomorph.2005.06.002, 2005.

Hutchinson, J.: Keynote paper: Landslide hazard assessment, in Landslides, edited by D. Bell, pp. 1805–1841, Balkema, A.A., Rotterdam., 1995.

INETI: Carta geológica da Área Metropolitana de Lisboa na escala 1:25000., 2005.

10 Jenness, J., Brost, B. and Beier, P.: Land Facet Corridor Designer: Extension for ArcGIS, [online] Available from: http://www.jennessent.com/arcgis/land_facets_htm, 2011.

Jeremias, F. T.: Geological Controls on the Engineering Properties of Mudrocks of the North Lisbon Area, Tese de Doutoramento, Department of Civil and Structural Engineering, University of Sheffield., 2000.

Lee, S., Ryu, J.-H. and Kim, I.-S.: Landslide susceptibility analysis and its verification using likelihood ratio, logistic 15 regression, and artificial neural network models: case study of Youngin, Korea, Landslides, 4(August 2006), 327–338, doi:10.1007/s10346-007-0088-x, 2007.

Lencastre, A. and Franco, F.: Lições de hidrologia, Fundação para a Ciência e a Tecnologia, Lisboa., 2006.

Montgomery, D., Sullivan, K. and Greenberg, H.: Regional test of a model for shallow landsliding, Hydrol. Process., 12, 943–945, 1998.

20 O' Loughlin, E.: Prediction of surface saturation zones in natural catchments by topographic analysis, Water Resour. Res., 22(5), 794–804, 1986.

O'Callagham, J. and Mark, D.: The extraction of drainage networks from digital elevation data, Comput. Vision, Graph. Image Process., 28(3), 323–344, 1984.

Oliveira, S. C.: Incidência espacial e temporal da instabildiade gemorfológica na bacia do rio Grande da Pipa (Arruda dos 25 Vinhos), Instituto de Geografia e Ordenamento do Território. Universidade de Lisboa., 2012.

Oliveira, S. C., Zêzere, J. L., Catalão, J. and Nico, G.: The contribution of PSInSAR interferometry to landslide hazard in weak rock-dominated areas, Landslides, 12(4), 703–719, doi:10.1007/s10346-014-0522-9, 2015.

Piacentini, D., Devoto, S., Montovani, M., Pasuto, A., Prampolini, M. and Soldati, M.: Landslide susceptibility modeling assisted by Persistent Scatterers Interferometry (PSI): an example from the northwestern coast of Malta, Nat. Hazards, 78, 30 681–697, doi:10.1007/s11069-015-1740-8, 2015.

Pimenta, R.: Avaliação da susceptibilidade à ocorrência de movimentos de vertente com métodos de base física, Faculdade de Ciências, Universidade de Lisboa., 2011.

Pradham, A. and Kim, Y.-T.: Application and comparison of shallow landslide susceptibility models in weathered granite soil under extreme rainfall events, Environ. Earth Sci., 73, 5761–5771, doi:10.1007/s12665-014-3829-x, 2015.

Rawls, W., Brakensiek, D. and Saxton, K.: Estimation of soil water properties, Trans. ASAE, 25(5), 1316–1320 and 1328, 1982.

Remondo, J., Bonachea, J. and Cendrero, A.: A statistical approach to landslide risk modelling at basin scale: From landslide susceptibility to quantitative risk assessment, Landslides, 2(4), 321–328, doi:10.1007/s10346-005-0016-x, 2005.

5 Sawatzky, D. L., Raines, G. L., Bonham-Carter, G. F. and Looney, C. G.: ArcSDM: ArcMAP extension for spatial data modelling using weights of evidence, logistic regression, fuzzy logic and neural network analysis., 2008.

Seefelder, C. de L. N., Koide, S. and Mergili, M.: Does parameterization influence the performance of slope stability model results? A case study in Rio de Janeiro, Brazil, Landslides, (November), doi:10.1007/s10346-016-0783-6, 2016.

Sharma, S.: Slope stability concepts, in Slope stability and stabilization methods, edited by L. W. Abramson, T. S. Lee, and

10 G. M. Sharma, S E, Boyce, pp. 329–461, John Wiley & Sons Inc., New York., 2002.

Sørensen, R., Zinko, U. and Seibert, J.: On the calculation of the topographic wetness index : evaluation of different methods based on field observations, Hydrol. Earth Syst. Sci., 10, 101–112, 2006.

Süzen, M. and Doyuran, V.: A comparison of the GIS based landslide susceptibility assessment methods : multivariate versus bivariate, Environ. Geol., 45, 665–679, doi:10.1007/s00254-003-0917-8, 2004.

15 Teixeira, M., Bateira, C., Marques, F. and Vieira, B.: Physically based shallow translational landslide susceptibility analysis in Tibo catchment , NW of Portugal, Landslides, 12, 455–468, doi:10.1007/s10346-014-0494-9, 2015.

Trigo, R. M., Zêzere, J. L., Rodrigues, M. L. and Trigo, I. F.: The Influence of the North Atlantic Oscillation on Rainfall Triggering of Landslides near Lisbon, Nat. Hazards, 36, 331–354, doi:10.1007/s11069-005-1709-0, 2005.

Vallejo, L., Ferrer, M., Ortuño, L. and Oteo, C.: Ingeniería Geológica, Pearson Educación, Madrid., 2002.

20 Varnes, D., Slopes, I. A. of E. G. and On, C. on L. and O. M. M.: Landslide hazard zonation: a review of principles and practice, edited by Unesco, Paris., 1984.

Visser, H. and Nijs, T.: The Map Comparison Kit, Environ. Model. Softw., 21, 346–358, 2006.

Yilmaz, I. and Keskin, I.: GIS based statistical and physical approaches to landslide susceptibility mapping (Sebinkarahisar , Turkey), Bull. Eng. Geol. Environ., 68, 459–471, doi:10.1007/s10064-009-0188-z, 2009.

25 Yin, K. L. and Yan, T. Z.: Statistical prediction models for slope instability of metamorphic rocks, in Landslides, edited by C. Bonnard, pp. 1269–1272, Balkema, Rotterdam., 1988.

Zbyszewski, G. and Assunção, C. T.: Notícia explicativa da folha 30-D (Alenquer). Carta Geológica de Portugal, Serviços Geológicos de Portugal, Lisboa., 1965.

Zêzere, J. L.: As costeiras a Norte de Lisboa: Evolução quaternária e dinâmica actual das vertentes, Finisterra, XXVI(51),

30 27–56, 1991.

Zêzere, J. L.: Landslide susceptibility assessment considering landslide typology . A case study in the area north of Lisbon (Portugal), Nat. Hazards Earth Syst. Sci., 2, 73–82, 2002.

Zêzere, J. L. and Rodrigues, M. L.: Rainfall Thresholds for Landsliding in Lisbon Area (Portugal), in Landslides, edited by J. Rybar, J. Stemberk, and P. Wagner, A.A. Balkema Publishers, Lisse., 2002.

Zêzere, J. L. and Trigo, R. M.: Impacts of the North Atlantic Oscillation on Landslides, in Hydrologicall, Socioeconomic and ecological impacts of the North Atlantic Oscillation in the Mediterranean Region, edited by S. Vicente-Serrano and R. Trigo, pp. 199–212, Springer., 2011.

Zêzere, J. L., Ferreira, A. B. and Rodrigues, M. L.: Landslides in the North of Lisbon Region (Portugal): Conditioning and Triggering Factors, Phys. Chem. Earth, 24(10), 925–934, 1999.

Zêzere, J. L., Trigo, R. M. and Trigo, I. F.: Shallow and deep landslides induced by rainfall in the Lisbon region (Portugal): assessment of relationships with the North Atlantic Oscillation, Nat. Hazards Earth Syst. Sci., 5, 331–344, 2005.

Zêzere, J. L., Vaz, T., Pereira, S., Oliveira, S. C., Marques, R. and Garcia, R. A. C.: Rainfall thresholds for landslide activity in Portugal: a state of the art, Environ. Earth Sci., 73(6), 2917–2936, doi:10.1007/s12665-014-3672-0, 2015.

Zizioli, D., Meisina, C., Valentino, R. and Montrasio, L.: Comparison between different approaches to modeling shallow Atmospheric landslide susceptibility : a case history in Oltrepo Pavese , Measurement Northern Italy, Nat. Hazards Earth Syst. Sci., 13, 559–573, doi:10.5194/nhess-13-559-2013, 2013.

Table 1. Shallow slides inventory characteristics and distribution per lithological units. Landslides affecting more than one lithological unit were considered within the dominant lithological unit.

ID	Parameters	Training group	Validation group	Total inventory
Total study area	# slides and density (#slides/km^2)	51 (3.7)	60 (4.3)	111 (8.0)
	Mean area (m^2)	533.9	495.7	513.2
	SD (slide area, m^2)	849.2	526.1	693.8
	Mean volume (m^3)	648.2	508.2	572.5
	SD (slide volume, m^3)	1929.2	818.6	1441.2
L1 Alluvium (Holocene)	No shallow slides inside the lithological unit			
L2 Limestones and marls (lower Thitonian)	# slides and density (#slides/km^2)	27 (5.0)	18 (3.3)	45 (8.3)
	Mean area (m^2)	635.7	446.8	560.1
	SD (slide area, m^2)	1063.2	365.6	860.4
	Mean volume (m^3)	859.1	396.5	674.1
	SD (slide volume, m^3)	2539.8	534.1	2008.9
L3 Sandstones and limestones (upper Kimmeridgian - Thitonian)	# slides and density (#slides/km^2)	2 (21.2)	5 (53.3)	7 (74.3)
	Mean area (m^2)	231.8	142.1	167.7
	SD (slide area, m^2)	155.5	120.5	137.6
	Mean volume (m^3)	151.3	78.8	99.5
	SD (slide volume, m^3)	124.5	92.0	107.5
L4 Mudstones and marly limestones (upper Kimmeridgian - Thitonian)	# slides and density (#slides/km^2)	8 (3.4)	16 (6.7)	24 (10.1)
	Mean area (m^2)	526.3	767.0	686.8
	SD (slide area, m^2)	696.3	754.3	744.2
	Mean volume (m^3)	614.2	936.5	829.1
	SD (slide volume, m^3)	1136.0	1279.7	1243.0
L5	# slides and density (#slides/km^2)	6 (2.6)	11 (4.8)	17 (7.4)

Limestones (upper Kimmeridgian)	Mean area (m^2)	449.4	336.4	376.3
	SD (slide area, m^2)	403.0	307.3	348.3
	Mean volume (m^3)	421.3	279.7	329.7
	SD (slide volume, m^3)	498.7	341.1	409.5
L6 Marls (upper Kimmeridgian)		No shallow slides inside the lithological unit		
L7 Mudstones and marls (Kimmeridgian)	# slides and density (#slides/km^2)	7 (2.1)	10 (3.0)	17 (5.2)
	Mean area (m^2)	373.1	501.6	448.7
	SD (slide area, m^2)	256.2	431.6	375.0
	Mean volume (m^3)	298.5	490.1	411.2
	SD (slide volume, m^3)	278.5	537.4	459.1
L8 Dykes and volcanic masses	# slides and density (#slides/km^2)	1 (6.8)		1 (6.8)
	Mean area (m^2)	81.0	No shallow slides inside the lithological unit	81.0
	SD (slide area, m^2)	0.0		0.0
	Mean volume (m^3)	29.1		29.1
	SD (slide volume, m^3)	0.0		0.0

Table 2. Description of landslide predisposing factor classes and respective Information Value scores (*Ii*)

Predisposing factor	ID	Description	# Pixels	# Pixels with landslides	*Ii*
Lithology	L1	Alluvium	2064	0	-1,760
	L2	Limestone and marls	217575	701	0,494
	L3	Sandstones and limestones	3771	20	0,993
	L4	Clays and marly limestones	95106	151	-0,213
	L5	Limestones	92363	96	-0,637
	L6	Marls	4331	7	-0,196
	L7	Clays and marls	131898	110	-0,857
	L8	Dykes and volcanic masses	5911	2	-1,759
Land Use	U1	Single species forest	12875	0	-2,187
	U2	Mixed forest	39044	100	0,265
	U3	Sclerophytic vegetation and poor natural pasturages	9319	0	-2,187
	U4	Low shrubs	27172	6	-2,186
	U5	High shrubs and degraded or transition forest	2792	29	1,665
	U6	Forest and annual agricultural areas	114403	240	0,065
	U7	Orchard and vineyards or mixed cultures	9113	0	-2,187
	U8	Annual agricultural areas and forest	13889	17	-0,474
	U9	Annual agricultural areas and vineyards	104697	144	-0,357
	U10	Olive grove and orchard or vineyards	1126	0	-2,187
	U11	Vineyards	56424	400	1,283
	U12	Vineyards and orchard	39126	30	-0,941
	U13	Complex cultural systems	104453	121	-0,529
	U14	Urban areas	18586	0	-2,187
Slope (°)	S1	0 – 5	71241	15	-2,234
	S2	5 – 10	207252	187	-0,779
	S3	10 – 15	156344	381	0,215
	S4	15 – 20	67852	157	0,163
	S5	20 – 25	27892	144	0,966
	S6	25 – 30	12284	74	1,120

	S7	30 – 35	5770	72	1,848
	S8	>35	4384	57	1,889
Aspect	A1	Flat	986	0	-0,886
	A2	North	82435	138	-0,161
	A3	Northeast	66693	349	0,979
	A4	East	99656	214	0,088
	A5	Southeast	69065	56	-0,885
	A6	South	33558	0	-0,886
	A7	Southwest	55920	75	-0,382
	A8	West	72192	94	-0,412
	A9	Northwest	72514	161	0,122
Profile slope curvature	C1	Convex (0,05 – 1,47)	190076	301	-0,216
	C2	Straight/Flat (-0,05 – 0,05)	128858	161	-0,453
	C3	Concave (0,05 – 1,22)	234085	625	0,306
Topographic Position Index (TPI)	T1	-21,23 – -12,49	5718	30	0,982
	T2	-12,49 – -7,53	30746	192	1,156
	T3	-7,53 – -2,57	130188	374	0,379
	T4	-2,57 – 2,39	210933	252	-0,498
	T5	2,39 – 7,35	115609	167	-0,308
	T6	7,35 – 31,83	59825	72	-0,491
Slope Over Area Ratio (SOAR)	R1	0	5052	10	0,007
	R2	0 – 0,00001	2261	12	0,993
	R3	0,00001 – 0,0001	4241	2	-1,427
	R4	0,0001 – 0,001	17928	30	-0,161
	R5	0,001 – 0,01	167668	240	-0,317
	R6	0,01 – 0,1	298168	590	0,007
	R7	> 0,1	57701	203	0,582

Table 3. K_c constant calibration parameter for each lithological unit

ID	Description	# Field soil measurement points	K_c
L1	Alluvium	0	2.9
L2	Limestone and marls	57	1.5
L3	Sandstones and limestones	0	3.6
L4	Clays and marly limestones	16	3.6
L5	Limestones	15	2.3
L6	Marls	1	2.9
L7	Clays and marls	21	4.3
L8	Dykes and volcanic masses	0	2.9

Table 4. Geotechnical parameters assigned to each lithological unit (LU). In brackets, cohesion and internal friction angle for each lithological unit to guarantee FS>1 in the absence of water into the soil (m=0).

ID	Specific soil weight (mean values)			Cohesion	Internal friction angle
	Saturated soil	Natural soil	Submerged soil		
	(kN/m³)	(kN/m³)	(kN/m³)	(kPa)	(°)
L1	17.5	16.5	7.69	3.0 (3.0)	19 (19)
L2	20.9	19.9	11.1	0.5 (1.0)	17 (27)
L3	20.6	19.6	10.8	2.0 (4.0)	16 (22)
L4	20.6	19.6	10.8	2.0 (4.0)	15 (19)
L5	20.9	19.9	11.1	1.5 (3.0)	24 (24)
L6	19.6	18.6	9.8	3.0 (3.0)	19 (21)
L7	19.6	18.6	9.8	2.0 (4.0)	19 (22)
L8	26.0	25.0	16.2	50.0 (50.0)	35 (35)

Table 5. Effective ratio of classes defined for the IV and IS shallow slide susceptibility maps

Susceptibility class	IV method			IS method		
	Class area	Landslide validation group area	Effective ratio	Class area	Landslide validation group area	Effective ratio
	(%)	(%)		(%)	(%)	
Very high	18.00	48.98	2.72	17.93	53.35	2.98
High	16.15	20.39	1.26	16.05	29.72	1.85
Moderate	14.02	11.74	0.84	14.06	11.66	0.83
Low	18.88	15.65	0.83	18.97	3.76	0.20
Very low	32.94	3.64	0.10	32.99	1.50	0.05

Table 6. Contingence table extracted from the overlay of IV and IS shallow slide susceptibility maps in % of the study area. Colours represent the susceptibility classes of the final map: Red – Very high; Orange – High; Yellow – Moderate; Light green – Low; Green – Very low; Grey – Uncertain, but with potential for high/very high susceptibility.

IS map\IV map	Very high	High	Moderate	Low	Very low	Total
Very high	8.0	3.9	2.2	2.0	1.1	17.3
High	4.5	3.9	3.0	2.9	1.8	16.1
Moderate	2.3	2.9	2.7	3.3	3.0	14.2
Low	2.1	2.9	3.1	4.6	6.5	19.2
Very low	1.2	2.2	3.0	6.2	20.7	33.3
Total	18.0	15.8	14.0	19.0	33.2	100

Table 7. Distribution (%) of shallow slides of the validation group in classes obtained by overlay IV and IS shallow slide susceptibility maps.

IS map\IV map	Very high	High	Moderate	Low	Very low	Total
Very high	24.8	12.0	3.6	9.1	2.6	52.1
High	18.8	5.7	2.5	2.6	0.4	30.0
Moderate	4.5	2.3	3.9	1.7	0.2	12.5
Low	0.9	0.3	1.7	1.0	0.0	3.8
Very low	0.0	0.0	0.2	1.3	0.1	1.5
Total	49.0	20.3	11.8	15.7	3.2	100

Table 8. Susceptibility classes and correspondent effective ratios of the final shallow slides susceptibility map

Susceptibility class	# Pixels	Unstable area (m^2)	Study area (%)	Unstable area (%)	Effective ratio
Very high	90786	18475	16.4	55.6	3.39
High	78678	6175	14.2	18.6	1.31
Moderate	50560	2400	9.1	7.2	0.79
Low	58456	425	10.6	1.3	0.12
Very low	184528	450	33.4	1.4	0.04
Uncertain – with potential to high or very high	90011	5300	16.3	16.0	0.98
Total	553019	33225	100	100	--
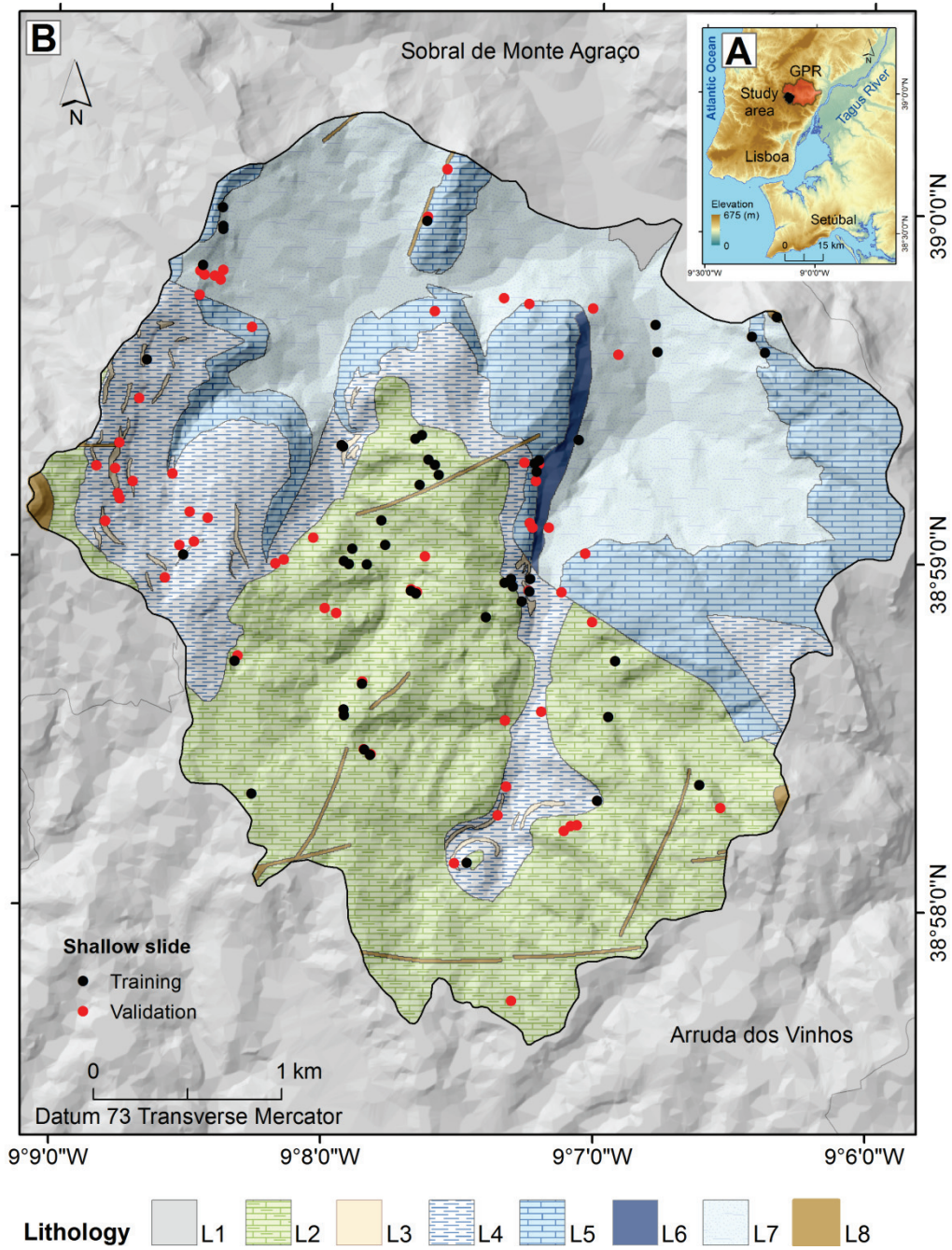
Figure 1: A) Location of Monfalim – Louriceira study area and **B)** spatial distribution of lithological units (L1 to L8): L1 - alluvium; L2 - limestones and marls; L3 - sandstones and limestones; L4 - clays and marly limestones; L5 - limestones; L6 - marls; L7 - clays and marls; L8 - dykes and volcanic masses. Shallow slides are represented as points.
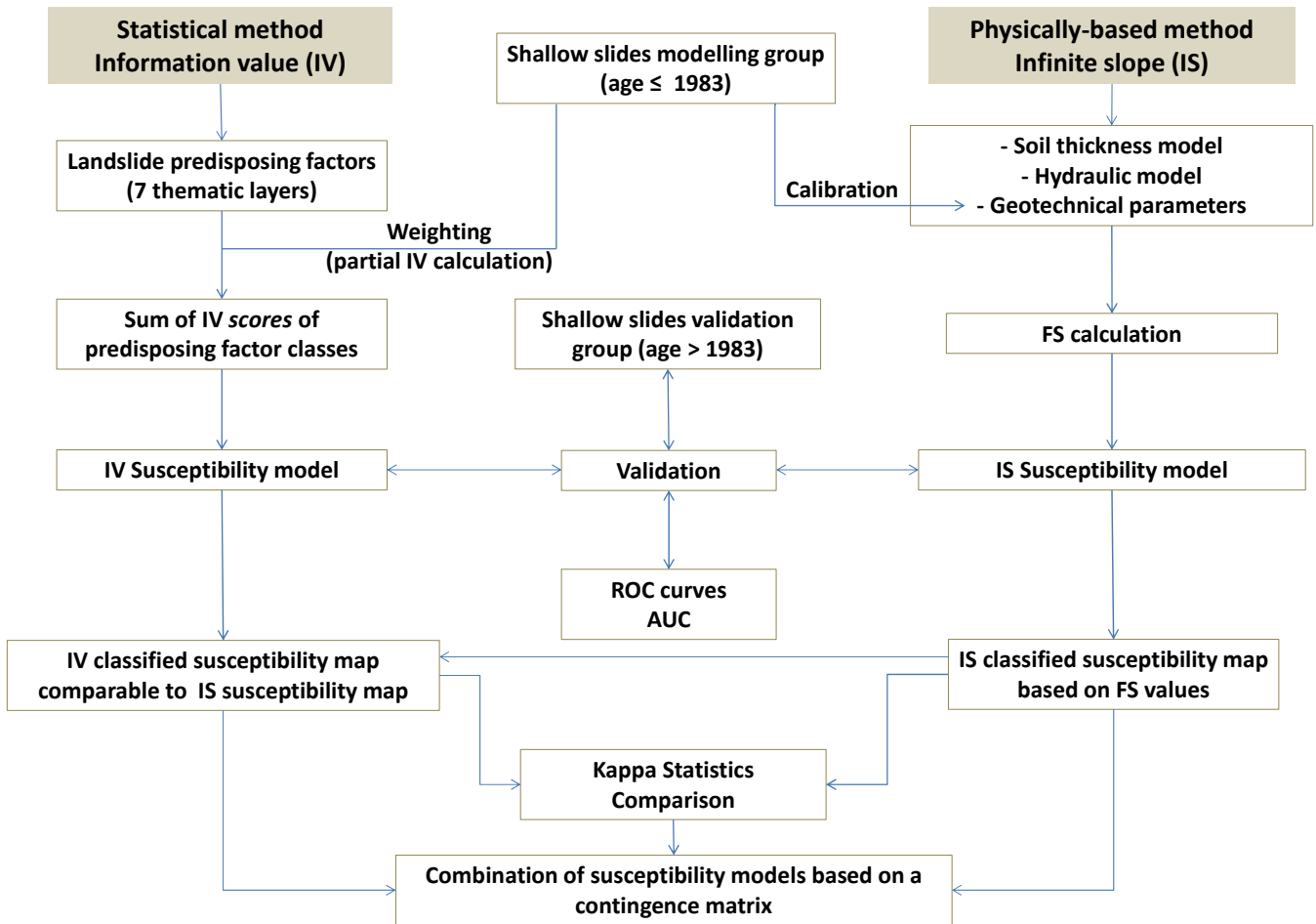
Figure 2: Methodological framework to compare and to combine statistical and physically-based landslide susceptibility models.
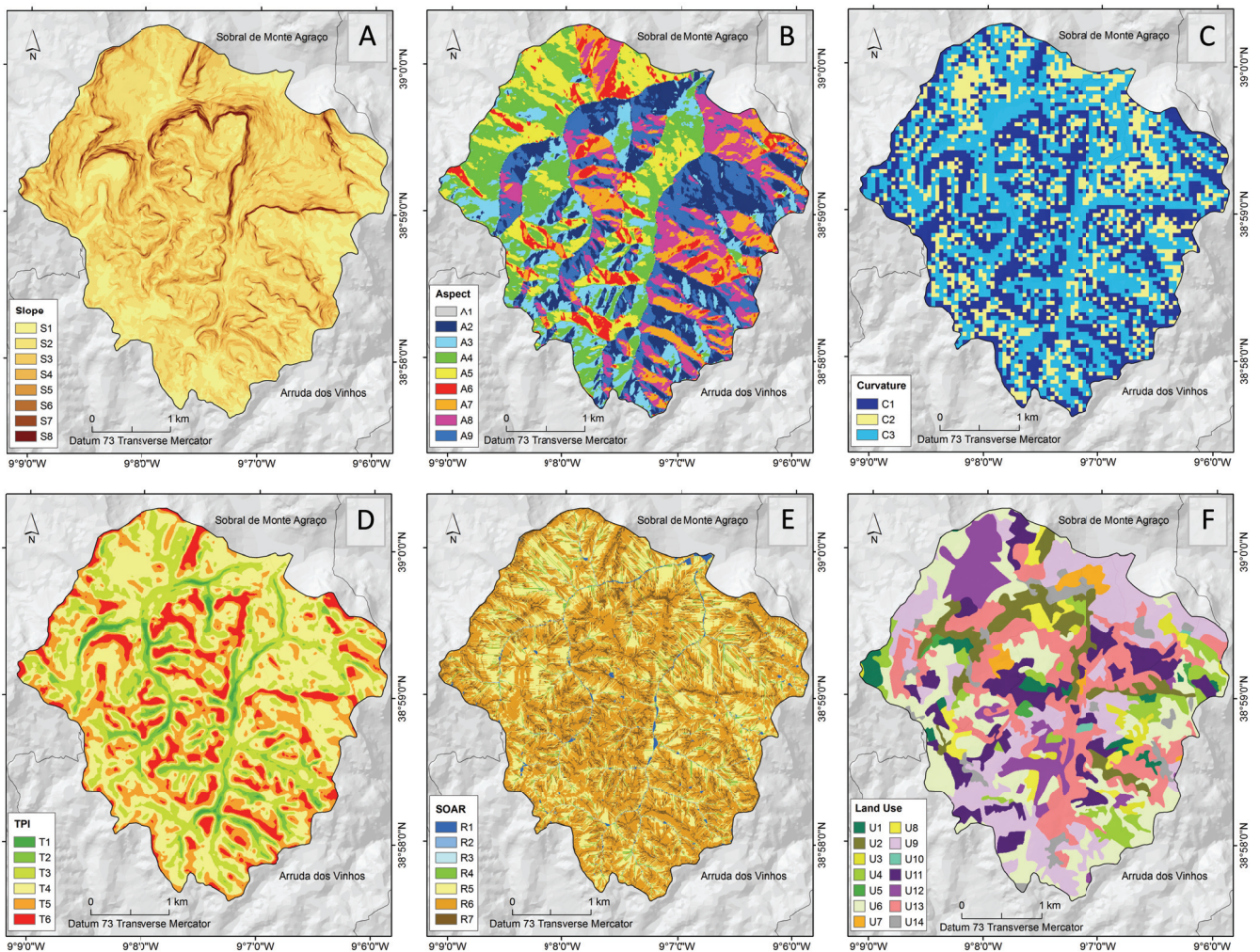
Figure 3: Dataset of shallow slides predisposing factors. A) slope, B) aspect, C) profile slope curvature, D) topographic position index, E) slope over area ratio, F) land use. Lithology is shown in Figure 1 and classes of landslide predisposing factor are described in Table 2.
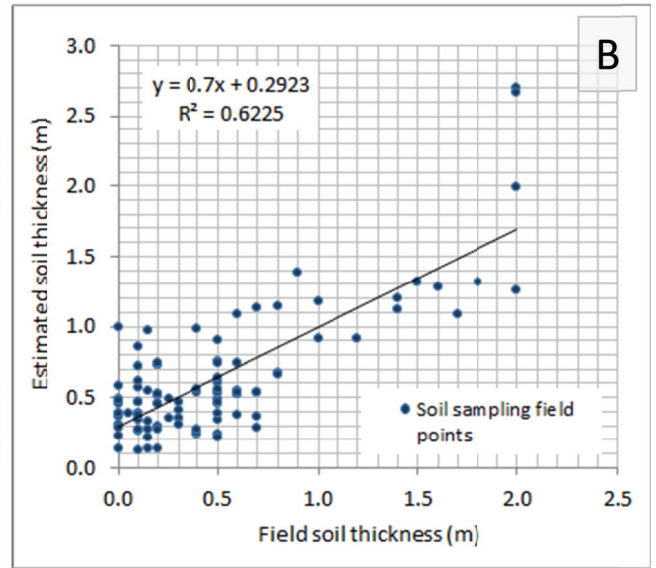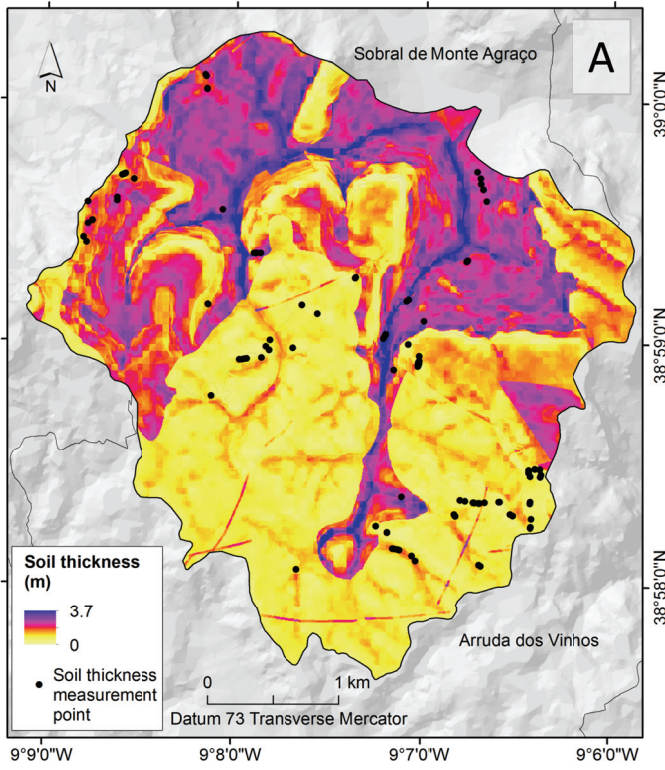
Figure 4: A) Soil thickness map; B) correlation between the field-measured soil thickness at sampling points and the estimated soil thickness. The eight sampling field points with more than one meter-error are not plotted.
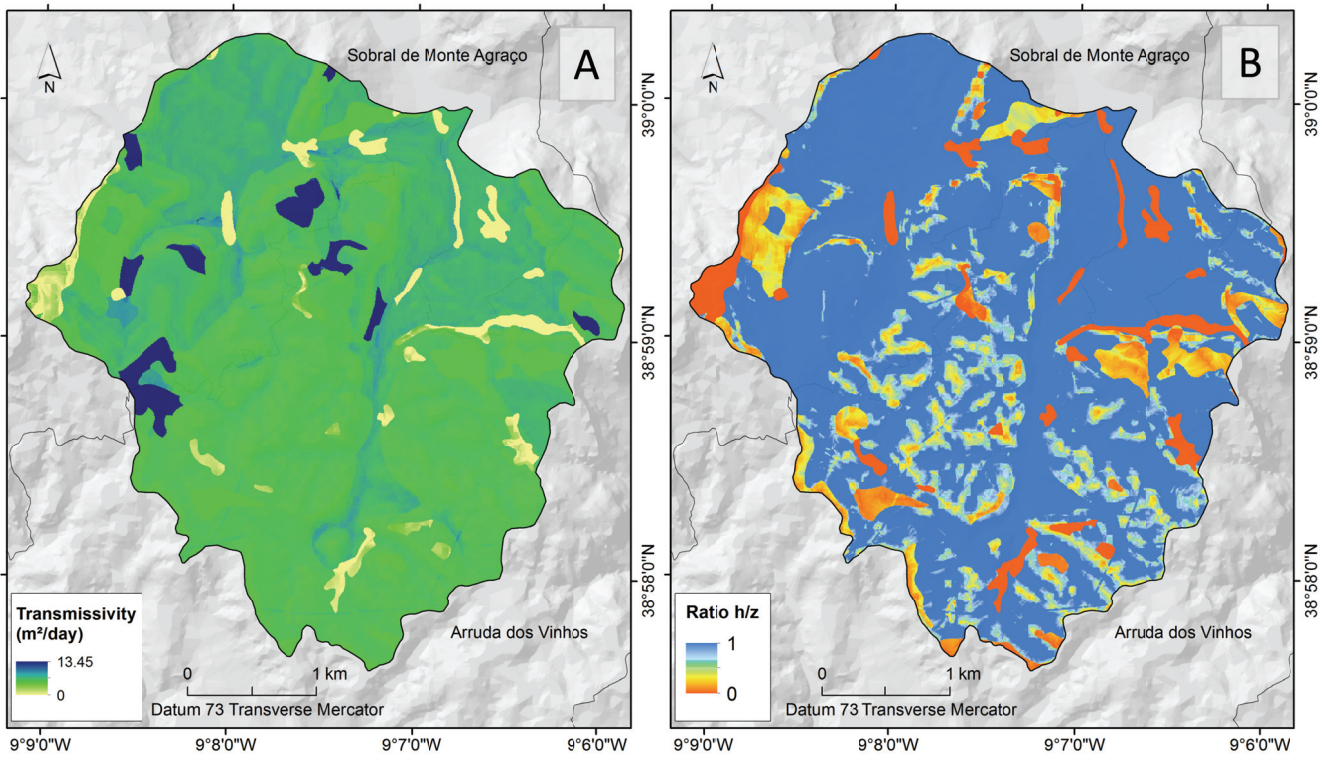
5   **Figure 5: Transmissivity (A) and ratio h/z (B) for the hydraulic model of the study area.**
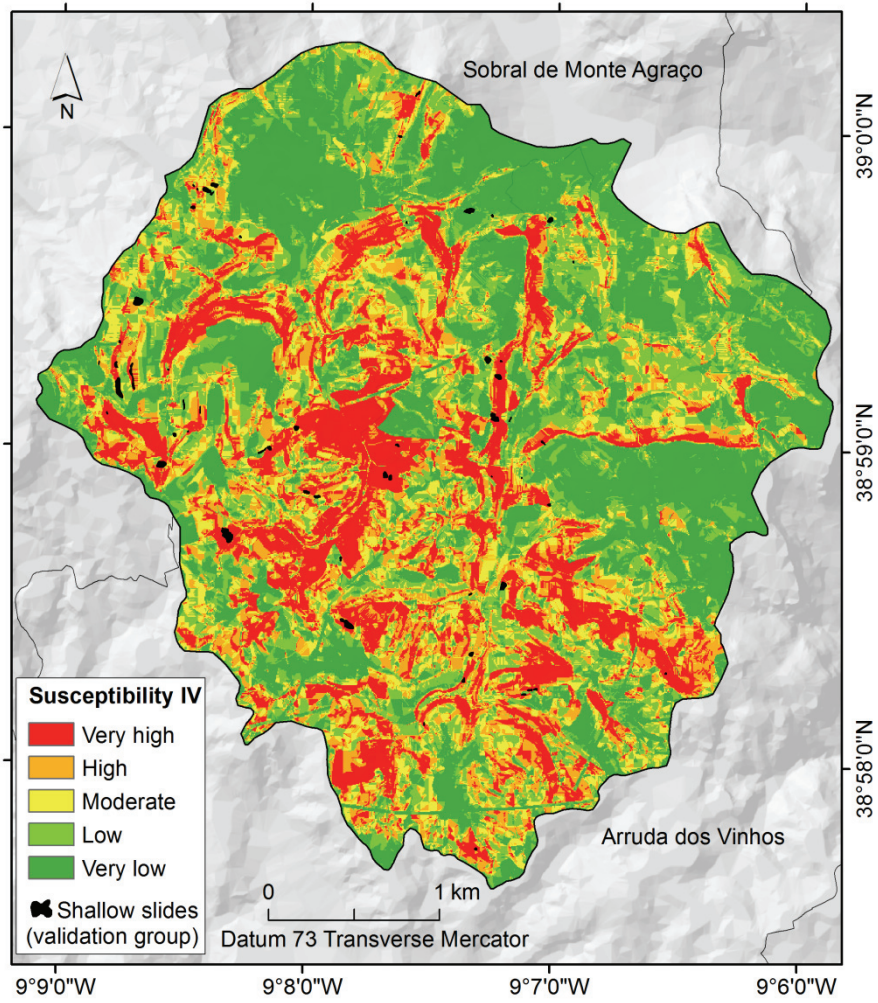
5   **Figure 6: IV Shallow slides susceptibility map.**
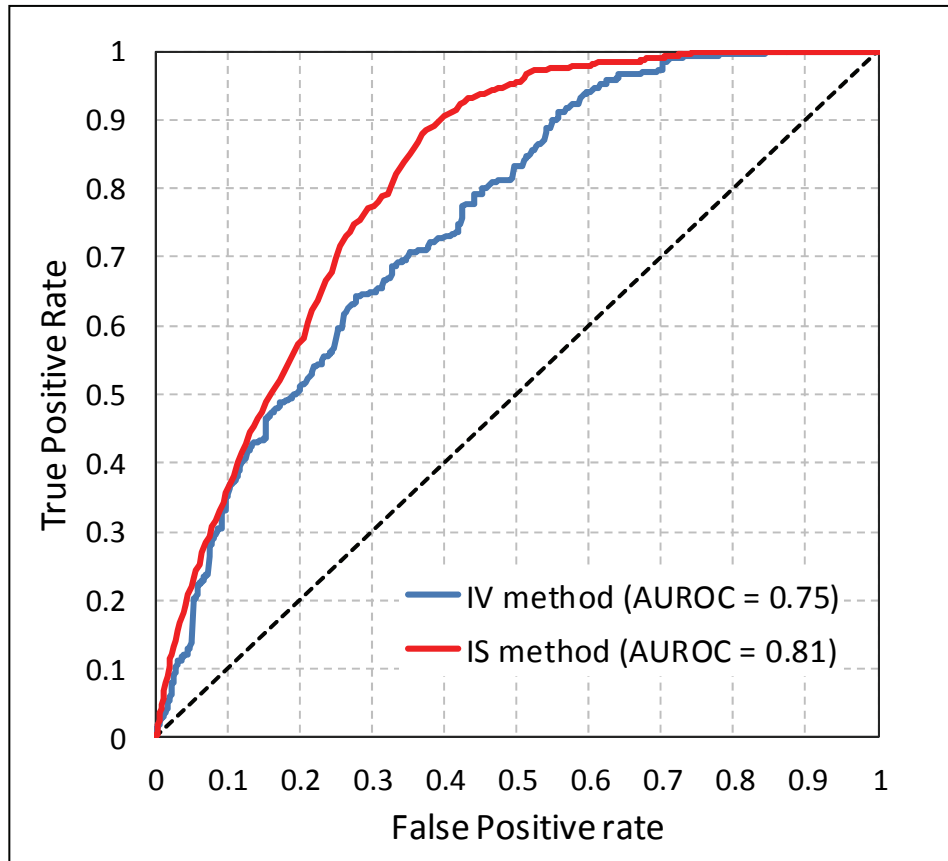
5   **Figure 7: ROC curves based on independent validation of IV and IS shallow slides susceptibility models.**
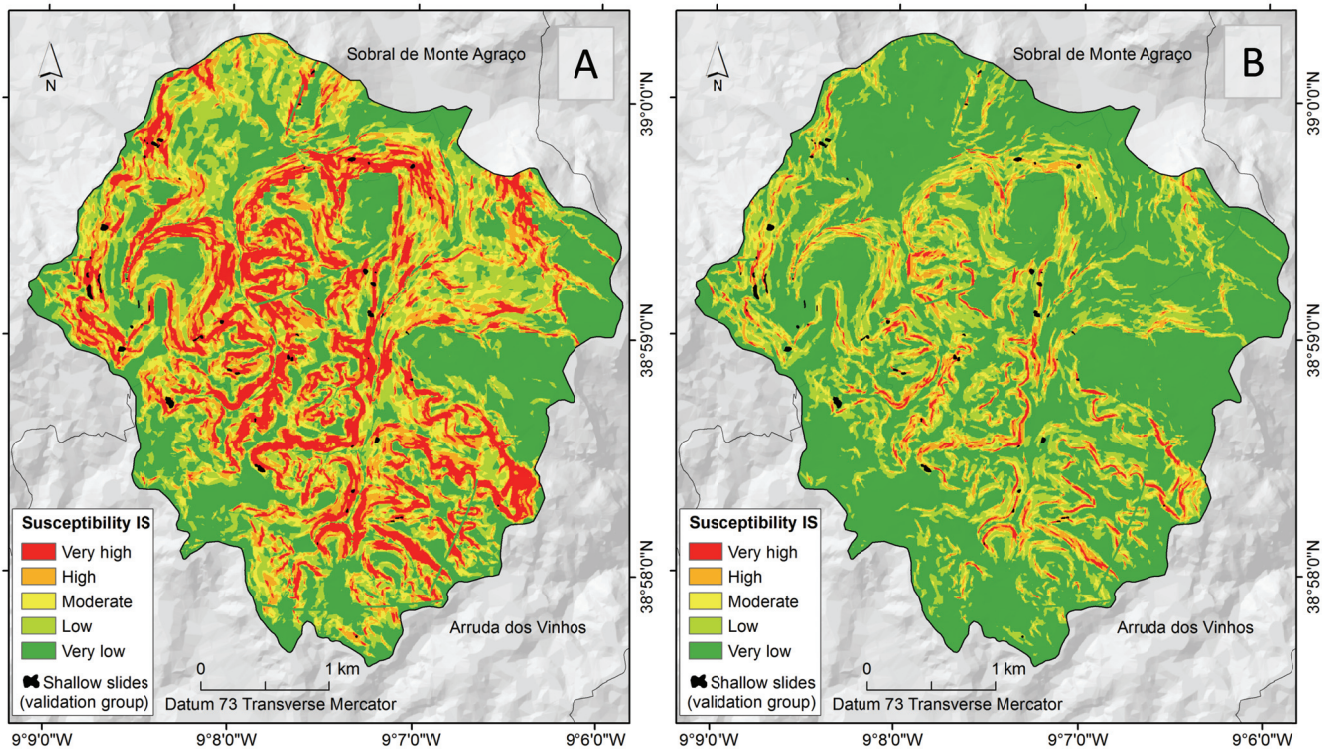
5   **Figure 8: IS shallow slides susceptibility maps (A) m according to figure 5b; (B) m = 0**.
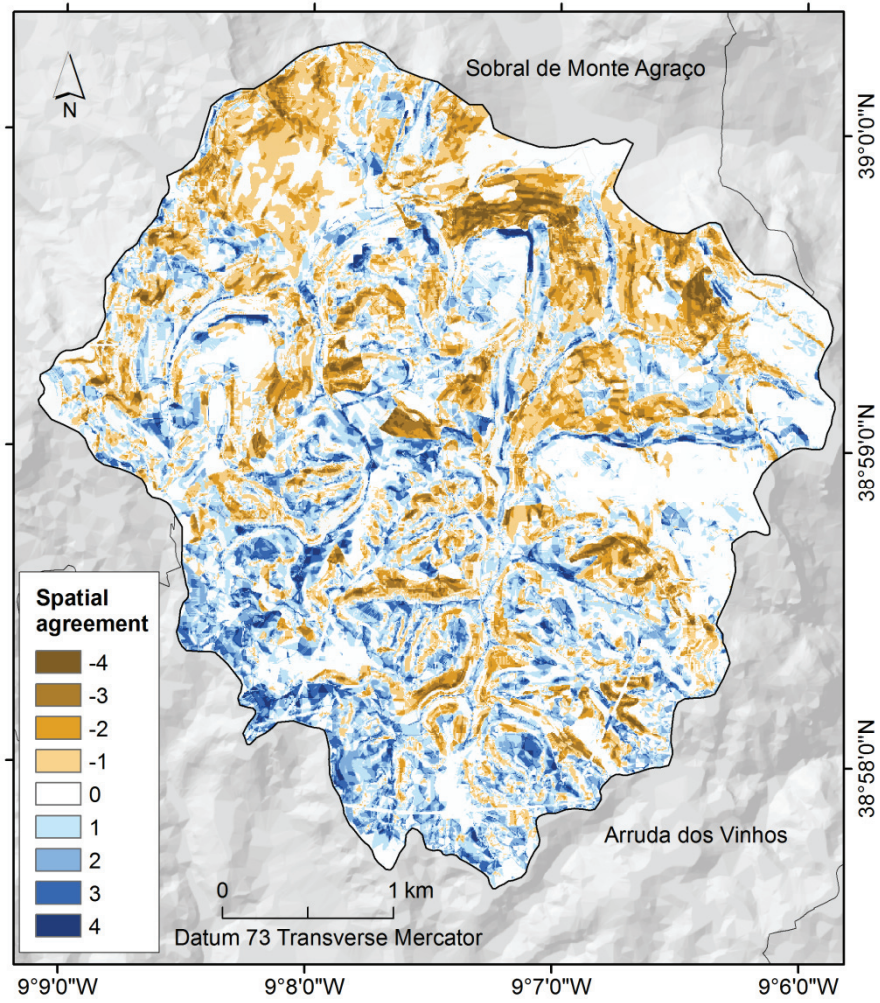
5 **Figure 9: Spatial agreement between IV and IS shallow slides susceptibility maps. 0 means full agreement; 4 and -4 means maximum disagreement.**
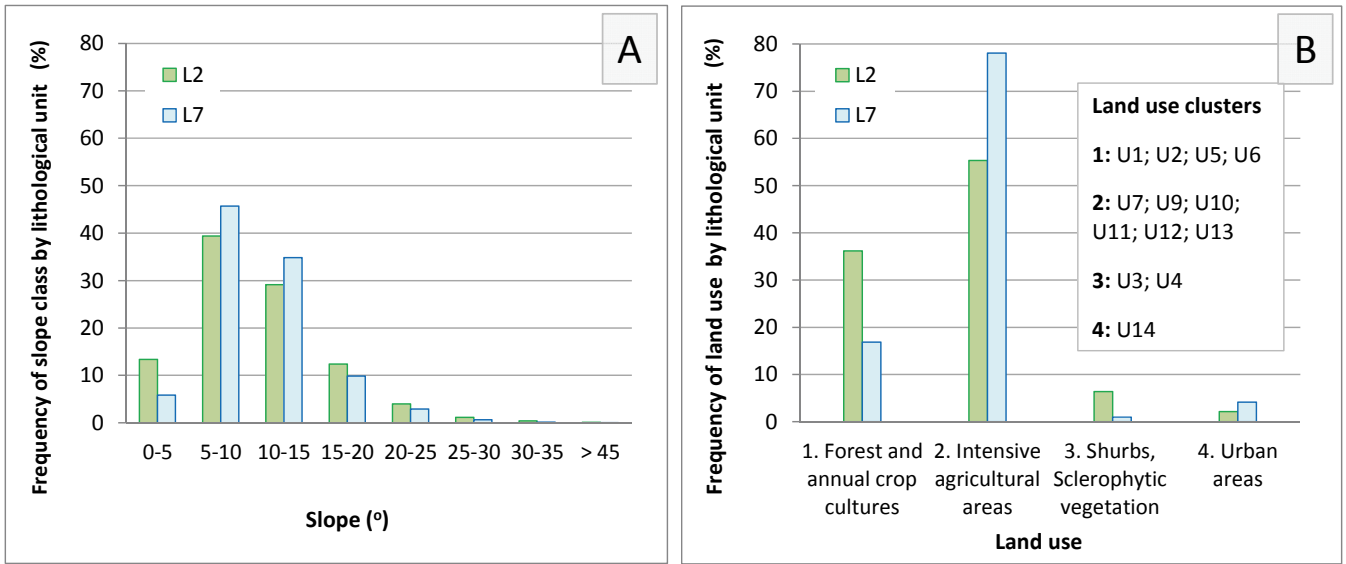
Figure 10: Frequency of slope A) and land use clusters B) within lithological units L2 and L7. Flat areas were not considered.
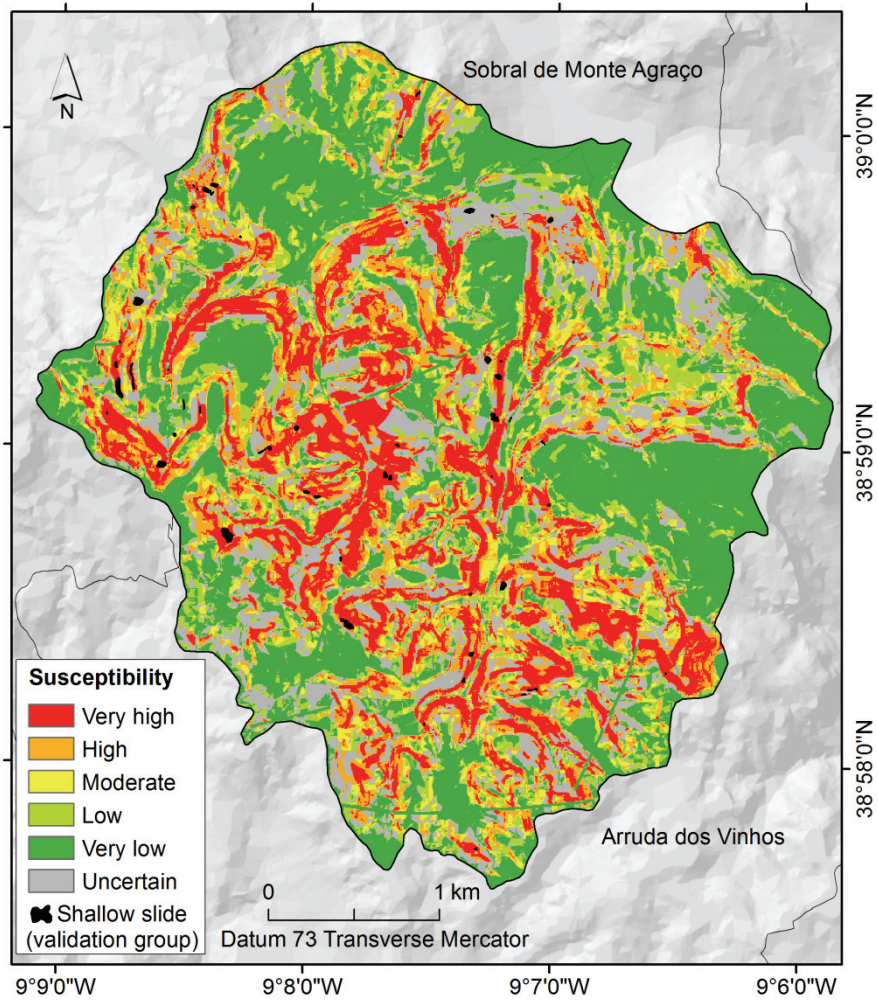
5   **Figure 11: Final shallow slides susceptibility map resulting from the combination of IV and IS susceptibility maps.**